Draft. Full paper at: http://dx.doi.org/10.1109/ICCP.2009.5284775

Automatic detection of liver capsule using Gabor filters. Applications in steatosis quantification

Cristian Vicas, Sergiu Nedevschi
Technical University Cluj Napoca, Romania
{cristian.vicas, sergiu.nedevschi}@cs.utcluj.ro

Monica Lupsor, Radu Badea
3rd Medical Clinic Cluj Napoca, Romania
{monica.lupsor, rbadea}@umfcluj.ro

Abstract

In this paper we present a new method of detecting hepatic capsule and other large structures from liver ultrasound images. Local texture anisotropy is evaluated using a specially designed bank of Gabor filters. We show that the proposed method is robust with respect to its parameters and is well suited for processing liver ultrasound images. Two human experts evaluate the method in conjunction with Canny edge detector and a method based on phase congruency. A practical application in quantifying the diffuse liver steatosis is presented. We show that proposed method can successfully replace the human expert in establishing the regions of interest used in steatosis quantification.

1. Introduction

Gabor filters belong to a larger class of methods that evaluate the local frequency spectrum of an image. They perform as a local band-pass filter with certain localization properties both in spatial and frequency domain [1]. They are mainly used to describe local features of an image for the purpose of classification and/or segmentation. It is believed that the Gabor filters simulate the behavior of human vision [2].

Medical ultrasound imaging produce images by reconstructing the echo amplitudes received from a previously excited tissue with a pulse of ultrasound waves. The usual frequencies used in clinical practice have a wavelength larger than the tissue cell sizes. In addition to that, in human tissue, the ultrasound wave suffers numerous effects of reflection, interference, scattering etc. The resulted images give only qualitative information about the underlying anatomical structures [3][4]. Simplicity and noninvasiveness make ultrasound investigation an excellent diagnostic tool, albeit one that depends more on the ability and experience of the examiner and is affected by many unstable factors [5]. Several studies focus on tissue characterization, which involves measuring the physical parameters of ultrasound images. The goal is to obtain quantitatively information on which a diagnosis can be based. In this paper we investigate liver steatosis.

The methodology of using ultrasound imaging as a quantitative diagnosis tool has several steps: first, is the acquisition process, followed by the establishment of some regions of interest (ROI). From these ROIs special designed algorithms numerically quantify various textural or non/textural properties and generate a feature set. By knowing the clinical diagnosis of the patient, researchers train a classification algorithm that will learn and hopefully predict the patient's diseases based on these feature sets. The first two steps are manually performed by trained physicians with inherited disadvantages (variability, low availability and error susceptibility).

This paper focuses on optimizing second step, the establishment of regions of interest. We propose an automated method that selects a special type of ROI used in quantifying steatosis. In our previous work [5],[6],[7],[8] we have developed algorithms that successfully describe and predict the liver steatosis. In conjunction with these algorithms we show that proposed method can replace a human expert in establishment of regions of interest.

Using Gabor filters [2] we propose a measure of the local texture anisotropy. Using this information one can decide if a texture region contains a feature (i.e. an anatomical structure, an artifact generated by shadowing or reflection etc) or contains only regular tissue echoes generated by homogenous liver tissue.

Using two trained physicians we evaluate the proposed method in conjunction with one classical edge detector (Canny) [9] and one other method used to detect local image features based on phase congruency [10]. We show that proposed method give the best results in terms of ROI establishment and we also show that the established ROIs gave comparable

detection performance with expert established regions of interest.

The paper is structured as following: in section 2 we give a short compendium on Gabor filters and in section 3 we present the principles behind the phase congruency. In section 4 is described the proposed method. Section 5 presents the experimental setup and the results on steatosis quantification. Discussions and conclusions to this paper are presented in section 6.

2. Gabor filters

2.1. Theoretical background

In spatial domain a Gabor filter is a product between a complex sinusoidal carrier and a 2D Gaussian shaped envelope: $g(x,y)=s(x,y)w(x,y)$ where *s(x,y)* is the complex sinusoid and *w(x,y)* is the Gaussian envelope [11],[12],[13],[14],[15],[16].

In spatial domain $s(x,y)=e^{j(2\pi(u_0x+v_0y)+P)}$ where (u_0,v_0) define the spatial frequency and *P* define the phase. If (u_0,v_0) represents a point in frequency space then they can be specified in polar coordinates in terms of F_0 and γ_0:

$$F_0=\sqrt{u_0^2+v_0^2},\ \gamma_0=\arctan\left(\frac{u_0}{v_0}\right).$$

Then *s(x,y)* becomes

$$s(x,y)=e^{i(2\pi F_0(x\cos\gamma_0+y\sin\gamma_0)+P)}, \quad (1)$$

where $i=\sqrt{-1}$. The gauss envelope is a simple 2D Gaussian function

$$w(x,y)=Ke^{-\pi(\frac{(x-x_0)_r^2}{A^2}+\frac{(y-y_0)_r^2}{B^2})}, \quad (2)$$

where

$(x-x_0)_r=(x-x_0)\cos\theta+(y-y_0)\sin\theta,$

$(y-y_0)_r=-(x-x_0)\sin\theta+(y-y_0)\cos\theta,$

and (x_0,y_0) are the coordinates for the peak of the Gaussian and θ is the rotation angle. *A* and *B* are standard deviations. In this paper the following conventions are assumed:

$$(x_0,y_0)=(0,0);\ \theta=\gamma_0;\ P=0;$$

$$F_0=\frac{1}{Period};\ K=\frac{2\pi}{AB},$$

where *Period* is the wavelength of the sinusoidal carrier. The definition of the Gabor kernel in spatial domain becomes:

$$g(x,y)=\frac{2\pi}{AB}e^{-\pi(\frac{(x\cos\theta+y\sin\theta)^2}{A^2}+\frac{(-x\sin\theta+y\cos\theta)^2}{B^2})}e^{i\frac{2\pi}{Period}(x\cos\theta+y\sin\theta)} \quad (3)$$

Knowing that

$$e^{ix}=\cos x+i\sin x, \quad (4)$$

s(x,y) can be decomposed in two parts, real and imaginary part.

As a result, in spatial domain, the complex Gabor function can be decomposed in two convolution kernels, $g_{re}(x,y)$ and $g_{im}(x,y)$.

By performing the Fourier transform on the Gabor function and expressing in polar coordinates one can compute the magnitude:

$$|G(u,v)|=2\pi e^{-\pi(A^2(u-u_0)^2+B^2(v-v_0)^2}} \quad (5)$$

where *G(u,v)* is the Fourier transform of *g(x,y)* and *|G(u,v)|* represents the magnitude of complex number *G(u,v)*.

As one can note, the magnitude of the response depends on frequency and orientation. It is possible to define a frequency and an orientation bandwidth. The bandwidth is usually computed in terms of half magnitude response.

The half-response is defined as the location in the frequency domain where the $|G(u,v)|=0.5|G(u_0,v_0)|$.

Usually the frequency bandwidth is measured in octaves. Let $F_{min}<F_0<F_{max}$ be the maximum and minimum frequencies such that

$$|G(u,v)|>=0.5|G(u_0,v_0|) \quad (6)$$

and

$$F_{\min}<=\sqrt{u^2+v^2}<=F_{\max} \quad (7)$$

The frequency bandwidth is defined as

$$\Delta F=\log_2\frac{F_{\max}}{F_{\min}} \quad (8)$$

where ΔF is expressed in octaves.

In a similar way is defined the angle bandwidth

$$\Delta\theta=\theta_{\max}-\theta_{\min} \quad (9)$$

where $\Delta\theta$ is expressed in radians.

From equation (5)-(9), one can compute that

$$\Delta F=\log_2\frac{F_0+\frac{1}{A}\sqrt{\frac{\ln 2}{\pi}}}{F_0-\frac{1}{A}\sqrt{\frac{\ln 2}{\pi}}}, \quad (10)$$

and

$$\tan(\frac{1}{2}\Delta\theta)=\frac{1}{BF_0}\sqrt{\frac{\ln 2}{\pi}}. \quad (11)$$

From the equations (10),(11) the terms *A* and *B* can be determined with respect to central angle, frequency and bandwidths:

$$A=\frac{1}{F_0}\sqrt{\frac{\ln 2}{\pi}}\frac{2^{\Delta F}+1}{2^{\Delta F}-1}, \quad (12)$$

and

$$B = \frac{1}{F_0}\sqrt{\frac{\ln 2}{\pi}}\frac{1}{\tan(\frac{1}{2}\Delta\theta)}. \quad (13)$$

By looking at equations (1),(2),(3),(12),(13) one can express a Gabor filter in terms of:

1/Period – central frequency response
θ_0 – central orientation response
ΔF – frequency bandwidth
$\Delta\theta$ – angle bandwidth

In actual applications a Gabor filter bank is used. Usually this filter bank is constructed in such a way that it will cover all frequency spectra by ensuring that the angle and frequency half-magnitude points of adjacent filters touch each other [16]. Let $F_{01} < F_{02}$ the central frequencies of two Gabor filters having the rest of the properties identical. We want to ensure that $F_{max1} = F_{min2}$ where F_{min} and F_{max} are the half peak magnitude frequency responses as defined in equations (6),(7),(8). Given the F_{01} and the ΔF the equation for computing F_{02} is

$$F_{02} = F_{01}\frac{1+\frac{2^{\Delta F}+1}{2^{\Delta F}-1}}{1-\frac{2^{\Delta F}+1}{2^{\Delta F}-1}}. \quad (14)$$

Let

$$R = \frac{1+\frac{2^{\Delta F}+1}{2^{\Delta F}-1}}{1-\frac{2^{\Delta F}+1}{2^{\Delta F}-1}}. \quad (15)$$

Using a recurrence formula one can compute the central frequency response of a filter bank by knowing the lowest central frequency, the frequency bandwidth and the desired number of frequency bands:

$$F_{0i} = F_{01}R^{i-1} \quad (16)$$

One major drawback for Gabor filters is that they have a DC response dependent on the filter frequency bandwidth.

$$DC_g = e^{-\sqrt{\frac{\ln 2}{2}}\frac{2^{\Delta F}+1}{2^{\Delta F}-1}} \quad (17)$$

Some DC corrections were investigated in [17]. The authors note that for small bandwidths (ΔF <0.7) the compensation is not needed.

2.2. Implementation details

Based on equation (4) the complex Gabor filter can be decomposed in two convolution kernels. By applying these two kernels on an image results the real and the imaginary response of the filter. In most papers the only significant value is the magnitude of the response:

$$\left|g(\Pi)\bullet I\right| = \sqrt{(g_{re}(\Pi)\bullet I)^2 + (g_{im}(\Pi)\bullet I)^2}$$

and $\Pi = (F_0, \theta_0, \Delta F, \Delta\theta)$

When generating the convolution in spatial domain kernels the width should be $W=k\cdot\max(A,B)$ where A and B are the standard deviations defined in equations (12),(13) and k should take values as 2.5 or 3 depending on the desired precision.

For large bandwidths and high frequencies the values for A and B are rather small thus the kernels are small. For small bandwidths and/or lower frequencies the kernels tend to become large. In these cases one should consider performing the convolution in Fourier space. Care should be taken when choosing the F_0 frequency in order to avoid aliasing [17].

3. Phase congruency

Morrone et. al. [18] has developed a model of feature perception. They claimed that the features are perceived at points in an image where the Fourier components are maximally in phase. In [10] Kovesi focuses on calculating the phase congruency as a dimensionless measure using a bank of log-Gabor filters. Based on this measure one could establish a threshold value independent of image contrast or dynamic range. He proposed the following formula (18) for the phase congruency:

$$PC(x) = \frac{\sum_o\sum_n W_o(x)\lfloor A_{no}(x)\Delta\Phi_{no}(x) - T_0\rfloor}{\sum_o\sum_n A_{no}(x) + \varepsilon}, \quad (18)$$

where

$$A_{no}(x)\Delta\Phi_{no}(x) = (e_{no}(x)\cdot\overline{\phi_e(x)} + o_{no}(x)\cdot\overline{\phi_o(x)}) - \left|e_{no}(x)\cdot\overline{\phi_o(x)} - o_{no}(x)\cdot\overline{\phi_e(x)}\right|,$$

$$W_o(x) = \frac{1}{1+e^{\gamma(c-s_o(x))}},\ s_o(x) = \frac{1}{N}\left(\frac{\sum_n A_{no}(x)}{\varepsilon + A_{\max o}(x)}\right),$$

$$A_{no}(x) = \sqrt{e_{no}^2(x) + o_{no}^2(x)},$$

$$\phi_{no}(x) = \arctan\left(\frac{e_{no}(x)}{o_{no}(x)}\right),$$

and $\lfloor x\rfloor = \max(x, 0)$.

T_o estimate the noise effect and is computed as:

$$T_o = \mu_r + k\sigma_r,$$

where

$$\mu_R^2 = \sigma_G\sqrt{\pi/2}\,,\ \sigma_r^2 = \frac{4-\pi}{2}\sigma_G^2\,,$$

$$\sigma_G^2 = |\hat{g}|^2\left(\Sigma\left(\sum_n M_n^2\right) + 2\Sigma\left(\sum_{i<j}(M_i M_j)\right)\right),$$

$$|\hat{g}|^2 \approx \frac{\Sigma(A_N^2)}{\Sigma(\hat{M}_N^2)},\ \Sigma(A_N^2) = \frac{-med(A_{No}^2)}{\ln 0.5},$$

and $e_{no}(x)/o_{no}(x)$ is the even/odd filter pair response of orientation o and frequency n at location x obtained with the convolution filter M_{no} and $F(f) = \hat{f}$ denote the Fourier transform. The expression $\Sigma(A)$ denote the expectance value for A.

The $A_{max\ o}(x)$ quantity denote the amplitude of the filter pair having maximum response at location x under orientation o. Variable c is a cutoff value for filter response spread below which the phase congruency values become penalized and γ is a gain factor that controls the sharpness of the cutoff. The variable n varies from 1 to N, and o varies from 1 to O, where N is the total number of frequency bands and O the total number of orientations being considered. The constant ε is added to prevent division by 0.

3.1 Log-Gabor filters

The log-Gabor filters are similar to Gabor filters but they have a logarithmic response in frequency direction and Gaussian response in angular direction [10],[17]. These filters do not have an analytical expression in spatial domain and the convolutions must be performed in the Fourier space [17]. The advantage of log-Gabor filters over simple Gabor filters is that they do not have a DC response. In Fourier space a log-Gabor filter is denoted by

$$LG(f,\theta) = e^{-\frac{\ln^2\left(\frac{f}{F_0}\right)}{2\ln^2(K_f)}} e^{-\frac{(\theta-\theta_0)^2}{2\Delta\theta^2}}, \quad (19)$$

$$K_f = e^{-\sqrt{\frac{\ln(2)}{2}}\Delta F},\ f = \sqrt{u^2+v^2},\ \theta = \arctan\left(\frac{u}{v}\right).$$

where F_0, Φ_0, ΔF, $\Delta\Phi$ have the same significance as in Gabor filters.

4. Proposed method

The main idea behind the proposed method is that in a region without any edges, the texture is relatively homogenous. In a region that contains an edge or other linear feature the texture presents an orientation, hence, anisotropy. Liver ultrasound images are characterized by a fine grained texture. This texture is not directly related to the liver tissue but to the interferences of ultrasounds on structures that have the dimension close to the ultrasound wavelength [3],[4].

The interfaces between larger structures and liver tissue have a different reflectivity and generate a larger echo. Because these structures have their own microstructures the interference pattern is still present. As a result, these structures generate fuzzy edges, sometimes these edges are marked only by a subtle texture difference or by a soft difference in luminosity. In addition to that, some authors claim that the grey level interference pattern follows a Rayleigh distribution [20]. Present method assumes that at anatomical interface locations the texture has a degree of anisotropy and tries to quantify this anisotropy.

Using a bank of oriented filters one can estimate the magnitude response of some frequency band as a function of orientation for each image location. For an isotropic texture the distribution of the response is fairly uniform. For an oriented texture there is a peak in the response at texture orientation. Computing the energy for the responses one could determine if there are peaks in the magnitude response.

The filter bank is implemented using Gabor filters. A central frequency along with a number of grade divisions is established. Let $Mag_i(x,y)$ be the magnitude response of filter i at location (x,y). Then,

$$\overline{Mag_i(x_w,y_w)} = \sum_{x,y}^{W} Mag_i(x+x_w, y+y_w)\,, \quad (20)$$

where W denotes the width of a square smoothing window of dimension aprox $A/2$ where A is the frequency stadnard deviation, as defined in equation (12) and (x_w,y_w) denote the window coordinates. These windows overlap by a factor of 0.25.

The energy can be computed as:

$$E(x_w,y_w) = \frac{\sum_o\left(\overline{Mag_o(x_w,y_w)}\right)^2}{\left(\sum_o \overline{Mag_o(x_w,y_w)}\right)^2}, \quad (21)$$

where o denotes the orientation.

For each pixel, the energy value is a linear combination between the energies of the windows that overlap the pixel. Each energy value is weighted according to the distance between current pixel and the center of the corresponding window. A threshold is applied to isolate the texture regions with high energy.

The method depends on some parameters. First we have to decide what frequency band (or bands) we

investigate. Second, a threshold must be established for the energy. If the energy is lower than selected threshold than the surrounding texture can be considered isotropic. The frequency band selects the dimensions of the features that we want to detect, and the threshold indicates the sensibility of the method.

Although several frequency bands can be used this is not recommended because at most of the natural textures the orientation is dependent of scale. The method is limited to linear or quasi-linear features because for a circular feature the proposed method will detect an isotropic texture. However, if the size of the feature is larger than the filter selection size, the feature's edges will get detected. Because of the band pass filter the smaller features will be ignored. As a result, it is possible that the texture has a strong orientation at finer scales and the proposed method will correctly detect larger features ignoring the finer scale anisotropy. Ultrasound images are characterized by this fine scale anisotropy because the resolution in axial direction is greater than the resolution in lateral direction [4],[20].

5. Experimental results

During investigation of liver steatosis a trained physician places several lines on ultrasound image. These lines should not intersect any large blood vessels or other artifacts and they should be traced from top liver capsule to bottom liver capsule (where visible).

As shown in our previous work [5],[6],[7],[8] the algorithms used for steatosis quantification are relatively robust. The goal of the proposed method is to replace the human component in ROI establishment. In this experiment, the ultrasound images were acquired using a convex transducer.

First step is the back-polar projection of ultrasound image (Figure 1). This ensures that adjacent pixels on horizontal or vertical axis have the same physical properties (are acquired from the same depth and have the same spatial and lateral resolution).

The second step is applying the proposed method (Figure 2). The third step projects the detected pixels back into the original image through a polar projection.

The coordinates of the polar projection depend only on transducer geometry and depth settings. The depth setting is set to 16 cm and kept constant through the image acquisition. As presented in previous chapter there are some parameters that need to be found. Two experts have independently scored (1 to 5) few sets of images. Each set consists of the same 16 ultrasound images. Each image belongs to a different patient in such a way that the entire diseases spectrum is covered.

The difference between various sets is the parameters used in detecting the liver capsule.

The quality criteria are the detection of liver capsule and the detection of major artifacts. There is no severe penalty if some liver texture gets selected in the process.

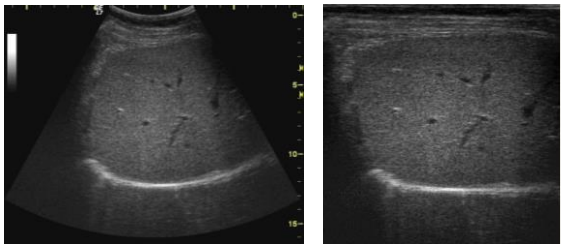

Figure 1.Original ultrasound image (left) and its inverse polar projection (right)

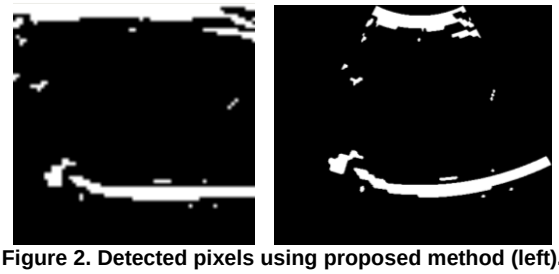

Figure 2. Detected pixels using proposed method (left). The detected pixels projected back into original image (right)

The number of orientations is fixed to 6 and the frequency bandwidth to 2. Angle bandwidth is set to 25 degrees. The central frequency and energy threshold are found using the experts. Few frequencies are proposed and the one with best score is selected. Then the threshold is selected for this frequency. In order to optimize the search of better values, a sort of coarse to fine strategy is used.

In Table 1 are shown the scores and the order that they were presented:

Table 1. The scoring from each frequency band.

Period	Expert 1 mean score	Expert 2 mean score
4	1.8	2.1
16	2.6	2.5
64	2.1	2.3
32	2.9	3.1
24	3.3	3.5

In Table 2 are shown the scores for the threshold. The central frequency is set to 1/24. As one can see the method is robust with respect to central frequency and threshold. A satisfying threshold has been rapidly found.

In addition to the proposed method, the ultrasound images were processed using a Canny edge detector

and an implementation of phase congruency. For Canny edge detector the tuned parameters were the hysteresis thresholds. For phase congruency, the filter bank, the gain and cutoff values were set as in [10].

Table 2. The scoring from each threshold value.

Threshold	Expert 1 mean score	Expert 2 mean score
0.01	1.8	2.1
0.1	2.1	2.9
0.3	2.7	3.1
0.5	2.8	2.5
0.2	3.4	3.6
0.15	3.8	3.7

The congruency threshold was the only variable selected into a similar manner as for proposed method. No satisfying parameter set could be found for Canny or for phase congruency.

In Figure 3 are shown the best results. In conclusion of these tests, only the proposed method was used in establishing the regions of interest for steatosis detection.

Both phase congruency and proposed method can generate information regarding the orientation. However, in this paper the non maximal suppression and hysteresis threshold were replaced by a simple threshold because the goal is to detect if there are artifacts present, not thinning their edges.

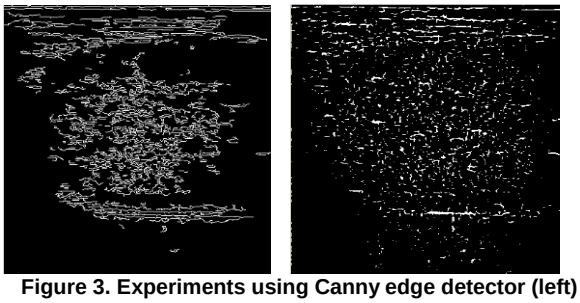

Figure 3. Experiments using Canny edge detector (left) and phase congruency (right)

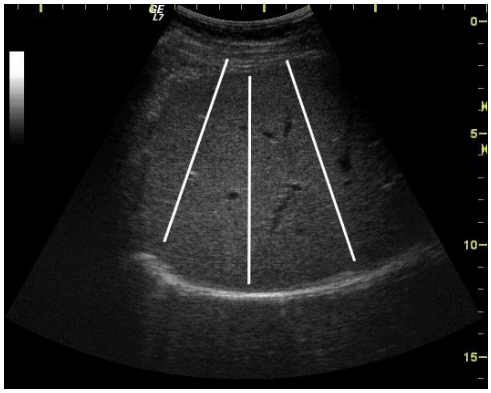

Figure 4. Three linear regions of interest established on the ultrasound image.

On each ultrasound image in the database 3-5 lines were randomly placed starting from the vertical center of the image as in Figure 4. If a line intersects a selected region the line is truncated. If the line has a length less than half of image depth (8 cm, approx. 150 pixels) than the line is rejected and a new one is searched. The search process ends after 10-20 tryouts.

On images with many artifacts is possible to select fewer lines. In most of the cases the proposed method does not perfectly detect the subcutaneous part of the liver capsule. However, because of the robustness of the features used to quantify the liver steatosis the proposed ROIs were accepted.

5.1 Steatosis detection

Attenuation and backscattering coefficients in conjunction with correlation coefficient and fit error are used to quantify the steatosis. The methodology is similar to our previous work [7]. The average gray level values for each point along the established line are calculated by averaging a certain number of pixels from left and right of this line (including the pixel beneath the line) [6],[7].

For each point of the line there were stored two values: the average gray level computed as above and the depth. Linear regression by least-squares approximation was applied to this dataset.

The slope represents the attenuation coefficient and the offset (intercept) represents the backscattering coefficient.

Two additional features were calculated, the correlation coefficient r^2 (22) and the fitting error s^2 (23).

$$r^2 = \frac{\sum_i (x_i - \bar{x})(y_i - \bar{y})}{\sum_i (x_i - \bar{x}) \sum_i (y_i - \bar{y})}. \quad (22)$$

$$s^2 = \sum \frac{(y_i - (a + b \cdot x_i))^2}{n - 2}, \quad (23)$$

where a is the offset and b is the slope of the linear regression. Variable n represents the number of pixels that are averaged to the left and right of the line is a parameter to the algorithm.

The slope, offset, r^2 and s^2 represent the output of the algorithm.

Given that one patient has more than one image, and each image can be fitted with up to 5 lines, a method of producing one feature set for each patient must be found. The simplest choice is by computing the mean for each value.

In this experiment were included 86 patients with NASH pathology. Ultrasound images are acquired from the right lobe at 16 cm depth. Brunt score, fatty infiltration grade and fibrosis stage are recorded after the liver biopsy. In addition, a group of 25 clinically healthy patients were investigated using only ultrasound (Table 3).

Table 3. The patients included in this study.

Steatosis grade	Number of patients
S0 (Healthy patients)	25
S1 (Mild steatosis)	32
S2 (Moderate steatosis)	37
S3 (Severe steatosis)	17

The patients were divided in three groups, according to the severity of the steatosis. Each group was submitted to a SVM classifier in a similar manner to our previous work [7]. In addition, a weighting parameter for the *Cost* was computed for each group in order to compensate for unbalanced data. Suppose that we have a dataset with two classes, each class has the volume n_1 and n_2. The cost weight for each class is c_1 and c_2. According to [19] the costs should be in the relation:

$$\frac{c_1}{c_2} = \frac{n_2}{n_1} \ . \qquad (24)$$

Let $n_2 > n_1$ and $c_2 = 1$. Then, $c_1 = \frac{n_2}{n_1}$.

The features were generated first using expert positioned regions of interest and then using the proposed method. The human expert establishes one region per ultrasound image.

Table 4. Experimental results for each dataset.

Dataset	Weights	Expert positioned ROIs AUC	Proposed method AUC
Healthy vs. steatosis patients (S0 vs. S123)	3.11 ; 1	0.87	0.84
Healthy and mild steatosis vs. patients with moderate and severe steatosis (S01 vs. S23)	1.05 ; 1	0.75	0.73
Non severe steatosis vs. severe steatosis patients (S012 vs S3)	1 ; 5.5	0.65	0.66

In both cases the mean was used to produce one feature set per patient. Using 10 fold cross validation the Area under Curve (AUC) vas recorded in each case. In Table 4 are shown the results.

Comparing current results with previous work one might note a decreased in performance. However, in [6],[7],[8] was generated one feature set per ultrasound image. As a result, the datasets were significantly larger than in current paper.

Some over fitting might also occurred, because after fold generation for cross-validation, the same patient could have feature sets present in both training and testing fold.

6. Conclusions

Some authors [4],[20] model the distribution of gray levels found in a US image as following a Rayleigh distribution. Using the Canny algorithm we model the fine texture as a Gaussian additive noise. As expected, Canny does not provide any useful results.

In theory phase congruency could be tuned to detect large features in the ultrasound image. In [10] phase congruency is applied on reflective images where the noise is additive and Gaussian. The ability to produce orientation information with arbitrary precision might allow phase congruency to produce thin edges even for features that have fuzzy and poorly localized edges. However, the experimental results don't support this theory.

More studies have to be performed on phase congruency method because is possible to tune the frequency response to log-Gabor filters in a similar manner as in proposed method. In [10] authors used large bandwidth kernels and enough frequency bands to cover the entire spectra. Limiting the bandwidth and eliminating the high frequency bands might reduce the method's sensibility to the noise usually found in ultrasound images.

The proposed method does not have a very good spatial localization. Depending on the threshold value the detected regions might shift. However, the value of threshold does not influence greatly the number or the shapes of detected features. From the expert supervised experiments resulted that a threshold value that varies from 0.1 to 0.3 gives a relatively uniform performance. Values greater than 0.05 select only very strong anisotropic regions (very rare in an ultrasound image). Values less than 0.5 select almost the entire image. We conclude that the method is relatively robust with respect to its main parameters.

Other combinations of central frequency and threshold might yield comparable (or superior) results. A search of these parameters is possible when we have an objective measurement of detected features.

Unfortunately this is a very hard desiderate to achieve because many times the experts disagree if certain feature on the US image is produced by an actual physical structure or is a shadowing artifact with no anatomical relevance. In addition to this, the poor spatial localization of the feature's edges rise another challenge in defining a measure for the detection performance.

The steatosis quantification rates obtained using proposed method to establish regions of interest are similar to those previously found using human expert. In conclusion, proposed method can be successfully employed to replace human component in establishing regions of interest on ultrasound liver image.

Further development in the direction of isolating the US image features (including liver capsule, major blood vessels, shadowing artifacts, etc) is achievable by tuning the frequency bands and creating complex rules for detecting each type of artifact. This will allow classification of the detected features (differentiation between liver capsule and a blood vessel).

Another important development direction is the study of the usefulness of this method when applied to other liver diseases (fibrosis, cirrhosis, focal lesions etc)

7. References

[1] P. Kruizinga, N. Petkov and S.E. Grigorescu, "Comparison of texture features based on Gabor filters," in *Proc. 10th Int. Conf. Image Analysis and Processing*, pp. 142-147, Sep. 1999.

[2]D. J. Field, "Relations between the statistics of natural images and the response properties of cortical cells," *J. Opt. Soc. Am. A*, vol. 4, no. 12, pp. 2379-2394, Dec., 1987.

[3] J. Jan , "Ultrasonography," in *Medical image processing, reconstruction and restoration: concepts and methods*, Ed. Boca Raton, FL: Taylor & Francis Group, 2006, pp. 283-334

[4] R. F. Wagner, S. W. Smith, J. M. Sandrik, H. Lopez, "Statistics Of Speckle In Ultrasound B-Scans," *IEEE Trans. Sonics And Ultrasonics*, vol. 30, pp. 156-163, May 1983.

[5] M. Lupsor, R. Badea, S. Nedevschi, C. Vicas, S. Tripon, H. Stefanescu, C. Radu, M. Grigorescu. "The Assessment Of Liver Fibrosis Using The Computerized Analysis Of Ultrasonographic Images. Is The Virtual Biopsy Appearing As An Option?," *Acta Electrotehnica*, Vol. 48 Nr. 4, Pp. 245-250, 2007

[6] C. Vicas, S. Nedevschi, M. Lupsor, R. Badea, M. Grigorescu "Steatohepatitis Detection from Ultrasound Images Using Attenuation and Backscattering Coefficients," *J. of Automation, Computers, Applied Mathematics*, vol. 16, no. 3, pp 20-26, 2007

[7] S. Nedevschi, C. Vicas, D. Mitrea M. Lupsor, M. Grigorescu, R. Badea, "Usefulness Of Attenuation And Backscattering Coefficients In Investigating Complex Nonalcoholic Steatohepatitis From Ultrasound Images. Preliminary Results," in *Proc. 19'th Biosignal Conference*, Brno , paper ID 126, Jun. 2008

[8]S. Nedevschi, C. Vicas, M. Lupsor, R. Badea, M. Grigorescu, "Usefulness of image processing techniques in assessing the diffuse liver diseases," in *Proc. ICCP 2008, 2nd Workshop Computers in Medical Diagnosis*, Cluj-Napoca, pp.10-15, Aug., 2008.

[9] R.C. Gonzales, R.E. Woods, *Digital Image Processing, 2-nd Edition*, Penitence Hall, 2002

[10] P. Kovesi, "Image features from phase congruency," J. Computer Vision Research, vol. 1, no. 3, pp. 2-27, 1999.

[11]J. R. Movellan. (2008,May 14). "Tutorial on Gabor Filters," [Online]. Available: http://mplab.ucsd.edu/tutorials/pdfs/gabor.pdf

[12] M. Lindenbaum, R. Sandler "Gabor Filter Analysis for Texture Segmentation," Technion, Comp. Science Dept. CIS-2005-05

[13] V. Levesque (2009, Apr, 25) Texture Segmentation Using Gabor Filters [Online]. Available: http://www.cim.mcgill.ca/~vleves/coursework.php

[14]A. Ahmadian, A. Mostafa, M. D. Abolhassani, Y. Salimpour, "A texture classification method for diffused liver diseases using gabor wavelets," in *Proc. 27th Ann. Conf. IEEE Engineering in Medicine and Biology*, pp. 1567-1570, 2005

[15]C. M. Chen, H. H-S. Lu, K-C. Han, "A Textural Approach Based On Gabor Functions For Texture Edge Detection In Ultrasound Images," *Ultrasound in Med. & Biol.*, Vol. 27, No. 4, pp. 515–534, 2001

[16] T. Randen, J. H. Husoy, "Filtering for texture classification: a comparative study," *IEEE Trans. Pattern Anal. Mach. Intell.*, vol. 21, no. 4, pp. 291 – 310, Apr., 1999.

[17]D. Boukerroui, J.A. Noble, M. Brady, "On The Selection Of Band-Pass Quadrature Filters," in *Frontiers in Robotics Research*, M.A. Denket Ed., Nova Science Publishers, Inc. pp. 69-112, 2006.

[18] M.C. Morrone, A. Navangione, D. Burr, "An adaptative approach to scale selection for line and edge detection," *Patt. Recog. Letters*, vol. 16, pp. 667-677, 1995

[19]C. W. Hsu, C. C. Chang, C. J. Lin. (2008, Oct. 2). "A practical guide to support vector classification," [Online]. Available: http://www.csie.ntu.edu.tw/~cjlin

[20]H. Yamada, M. Ebara, T. Yamaguchi, S. Okabe, H. Fukuda1, M. Yoshikawa, T. Kishimoto, H. Matsubara, H. Hachiya, H. Ishikura, H. Saisho "A pilot approach for quantitative assessment of liver fibrosis using ultrasound: preliminary results in 79 cases," *J. Hepatology*, vol. 44, pp. 68–75, 2006.